




# Predictive Value of Current Perception Threshold for Prognosis of Pulsed Radiofrequency in Patients with Acute Herpetic Neuralgia

Chengcheng Zhao <sup>1,2</sup>, Ziwei Lu<sup>1,2</sup>, Bohan Hua<sup>1,2</sup>, Jiayu Yue <sup>2</sup>, Qinru Yang<sup>2</sup>, Huadong Ni<sup>2</sup>, Ming Yao <sup>2</sup>

<sup>1</sup>Jiaxing University Master's Degree Cultivation Base, Zhejiang Chinese Medical University, Jiaxing City, Zhejiang Province, People's Republic of China;

<sup>2</sup>Department of Anesthesiology and Pain Research Center, The Affiliated Hospital of Jiaxing University, Jiaxing City, Zhejiang Province, People's Republic of China

Correspondence: Ming Yao, Email [jxyaoming@zjxu.edu.cn](mailto:jxyaoming@zjxu.edu.cn)

**Objective:** This study aimed to evaluate the prognostic accuracy of the Current Perception Threshold (CPT) in Acute Herpetic Neuralgia (AHN) patients receiving Pulsed Radiofrequency (PRF) therapy and to develop a corresponding prognostic model.

**Methods:** We retrospectively analyzed data from 106 AHN patients treated with PRF between January 2022 and May 2023. The occurrence of Postherpetic Neuralgia (PHN) after treatment categorized patients into non-PHN and PHN groups. The predictive role of CPT indices for PRF outcomes was assessed using the Receiver Operating Characteristic (ROC) curve and Area Under Curve (AUC). Then the dataset was split into a training set (n=74) and a validation set (n=32). Factors associated with PHN development were identified using univariate and multivariate logistic regression. A nomogram model was developed using significant predictors and internal validation was performed using valid set data.

**Results:** Among the 106 patients, 45 had a poor prognosis. Significant differences in age, preoperative Numerical Rating Scale (NRS) score, and 5Hz CPT ratio were observed between the groups ( $p < 0.05$ ). Logistic regression identified these factors as independent predictors for PRF prognosis ( $p < 0.05$ ). The 5Hz CPT ratio demonstrated predictive value (AUC= 0.764, 95% CI: 0.674–0.855). The nomogram model, incorporating these predictors, showed high AUC in both the training (0.863, 95% CI: 0.776–0.950) and validation sets (0.859, 95% CI: 0.721–0.998). Calibration curves indicated good model fit, and the Hosmer-Lemeshow test confirmed this ( $p > 0.05$ ). Decision Curve Analysis (DCA) highlighted the model's predictive advantage.

**Conclusion:** The 5Hz CPT ratio can predict the prognosis of PRF in AHN patients. The nomogram model has high precision and clinical utility. It can help identify AHN patients with a poor PRF prognosis at an early stage and assist in clinical decision-making.

**Keywords:** current perception threshold, neuralgia, postherpetic, pulsed radiofrequency treatment, predictive model

## Introduction

Herpes Zoster (HZ) is a disease caused by the reactivation of the Varicella Zoster Virus (VZV) that lies dormant in the sensory ganglia of the body.<sup>1</sup> It typically affects a single ganglionic segment and presents as clusters of herpes accompanied by severe pain in the skin of the corresponding area.<sup>2–4</sup> The thoracic back is the most commonly affected area, accounting for approximately 50–70% of cases.<sup>5</sup> Herpetic neuralgia (HN) can manifest as pinprick, electric shock, or burning pain. The disease course distinguishes acute herpetic neuralgia (AHN), subacute herpetic neuralgia (SHN), and postherpetic neuralgia (PHN). PHN is a severe complication of viral infection affecting peripheral nerves, causing typical neuropathic pain. Approximately 10–25% of patients experience pain lasting over a year. PHN is more common in patients over 50 years of age who are immunocompromised with diabetes mellitus and have extensive lesions and severe pain in the acute phase.<sup>6</sup> Numerous studies have shown that long-term chronic pain can lead to anxiety, depression, and even suicidal thoughts, which can be a heavy burden on both the family and society.<sup>7–9</sup>

Currently, the primary therapeutic approach for AHN involves drug therapy. Pregabalin, an ion channel blocker, is the first-line drug used in clinics.<sup>10</sup> However, drug therapy is ineffective for 20–40% of patients.<sup>11</sup> For patients with poor

drug efficacy, minimally invasive surgery is a commonly used treatment option. Pulsed Radiofrequency (PRF) is a minimally invasive neuromodulation technique that has been demonstrated to be a safe and effective method of controlling HN.<sup>12</sup> Furthermore, it has been shown that PRF not only achieves significant pain relief but also does not cause nerve damage.<sup>13</sup> Although PRF has demonstrated significant advantages in the treatment of HN, PHN still occurs in approximately 16% of patients after surgery.<sup>14</sup> Therefore, it is necessary to identify these patients early.

The Current Perception Threshold (CPT) is a quantitative assessment of sensory nerve function that is non-invasive, easy to operate, objective, and accurate. Three distinct frequencies of current stimulation were employed to quantitatively assess peripheral nerve function. CPT 2000 Hz was utilized to detect the function of large-diameter myelinated nerve fibers (class A $\beta$ ), which innervate light touch and pressure sensations. CPT 250 Hz was employed to assess the function of small-diameter myelinated nerve fibers (class A $\delta$ ), which conduct Fast nociceptive, temperature and pressure sensations, and CPT 5 Hz was used to detect the function of unmyelinated nerve fibers (class C) innervating temperature, slow nociception and innervating autonomic functions. Therefore, CPT is capable of detecting all types of nerve fiber damage at an early stage. It has been widely utilized in various fields such as Parkinson's disease, diabetic peripheral neuropathy, and spinal diseases.<sup>15–17</sup> Studies have demonstrated its utility in diagnosing diseases, evaluating treatment effectiveness, and forecasting outcomes.<sup>18</sup>

Although there is an emerging association between damage to sensory nerve fibers and the onset of HN, limited research has explored whether the extent of sensory nerve damage correlates with the prognosis of PRF therapy in patients with AHN. Therefore, the objective of this investigation was to assess the predictive capacity of CPT for PRF therapy and develop a clinical prognostic model for AHN patients, aiming to offer insights for tailored treatment strategies.

## Materials and Methods

### Patients

A total of 106 patients with AHN of the thoracic spine who received PRF treatment at the Pain Department of Jiaying University Hospital from January 2022 to May 2023 were included in the study. The inclusion criteria were as follows: meeting the diagnostic criteria for herpes zoster, having the infection located on the chest and back, being aged between 25 and 85 years, having a disease duration of less than one month, and having received ineffective medication for at least one week. The exclusion criteria encompassed individuals with chronic pain in the affected area, those with comorbidities such as diabetes mellitus or peripheral nerve entrapment syndrome that could cause spinal cord or peripheral nerve damage, patients unwilling to undergo neurophysiological tests, and those who declined to participate in follow-up or provide clinical information. The research protocol adhered to by the study was reviewed and approved by the Ethics Committee of the affiliated hospital of Jiaying University (2023LY571). Informed consent was obtained from all participants in accordance with the Declaration of Helsinki.

### Observations and Follow-Up

In this study, general demographic data such as gender, age, herpes side, disease duration(day), body mass index (BMI), hypertension, numeric rating scale (NRS) score, number of lesioned ganglion segments, and preoperative CPT examination data were all recorded. To represent the degree of sensory nerve function impairment, the CPT ratio of the affected side to the healthy side at different frequencies was used, considering the variability in CPT values among individuals. Following discharge, patients were monitored monthly for a period of 3 months. Persistence of pain at the herpes site after this 3-month period was defined as PHN. Patients were then categorized into either a non-PHN group or a PHN group, based on the development of PHN, which was considered a poor prognostic indicator.

### Pulsed Radiofrequency Treatment

All patients enrolled in this study underwent standard PRF treatment, which was performed by an experienced pain physician. The patients were positioned on the CT table with pillows placed beneath the abdomen, and the proposed nerve blocks and puncture points were identified according to the location of the skin lesions and pain sites. The procedure commenced with routine disinfection and local anesthesia. A puncture point was then made with radiofrequency trocars, followed by a CT-guided puncture to the affected side of the intervertebral foramen of the upper one-

third. The core of the needle was then extracted, and supporting electrodes were inserted along the trocars. Once the optimal position for the needle tip has been determined, the radiofrequency temperature should be adjusted to 42°C, with a duration of 300 seconds, a pulse duration of 40 milliseconds, a pulse frequency of 2 hz, and four cycles of pulse radiofrequency regulation. Once the radiofrequency treatment was complete, the needle core was removed, and a bandage was applied at the puncture site. The patient was observed for a period of fifteen minutes, after which he was returned to the ward if his vital signs remained stable.

## CPT Examination

The Neurometer<sup>®</sup> CPT/C Sensory Nerve Quantification Tester is employed in conducting the CPT assay. Before conducting the test, the room temperature is carefully controlled within the range of 20°C to 24°C. The patient's skin is sterilized and allowed to rest quietly for 15 minutes to prepare. Subsequently, the electrode sheet of the Quantitative Sensory Nerve Detector is positioned in the distribution area corresponding to the nerve endings affected by the patient's rash. The patient's body is then divided into two sides – the healthy side and the affected side – with the body's midline serving as the boundary. Once the patient is briefed on the test procedure, they are handed the control button to operate. The patient is instructed to release the button promptly upon feeling pinprick-like stimulation. The instrument automatically displays the current size upon release of the button, providing both the real stimulation size and the blank pseudo-stimulation size to the patient multiple times. The patient must accurately identify the real stimulation five times consecutively to complete the cycle; failure to do so results in the instrument increasing the stimulation intensity. This process is repeated in a cyclic manner. The minimum CPT values on both the affected and unaffected sides of the patient are then recorded at three different frequencies: 2000 hz, 250 hz, and 5 hz. The CPT ratio was calculated based on the CPT values.

## Statistical Analysis

The statistical analysis was conducted using R 4.2.3 software. The normality of the data was assessed using the Shapiro–Wilk test and histogram. For normally distributed continuous data, mean  $\pm$  standard deviation (SD) was used, while median and interquartile range (IQRs) were used for non-normally distributed continuous data. Categorical data were presented as numbers and percentages (%). Independent *t*-tests were employed for normally distributed continuous data, Mann–Whitney *U*-tests for non-normally distributed continuous data, and chi-square tests for categorical data. Then the data were randomly divided into a training set (n=74) and a validation set (n=32) at a ratio of 7:3. Variables such as patients' gender, age, disease duration, comorbid hypertension status, preoperative NRS score, and various CPT ratios were included in the univariate analysis. Independent variables with  $p < 0.2$  in the univariate analysis were then used in the multivariate logistic regression analysis to identify influencing factors of PRF prognosis in patients with AHN.  $p < 0.05$  indicated statistical significance. The predictive ability of CPT for PRF prognosis in patients with AHN of the thoracic back was evaluated through the Receiver Operating Characteristic (ROC) curve. A nomogram model was developed by selecting variables from multifactor logistic regression results. The area under the ROC curve, calibration curve, and Decision Curve Analysis (DCA) were utilized to assess model sensitivity, specificity, and clinical utility. Lastly, the model was internally validated using data from the validation set.

## Results

### Comparison of General Information

Of the 106 patients who completed the follow-up period, 45 patients continued to develop PHN after PRF. When comparing the demographic data of patients with different prognoses, it was found that the differences between the PHN (n=45) and non-PHN (n=61) groups concerning sex, comorbid hypertension, disease duration, BMI, number of ganglion segments involved, side of the rash, 2000Hz CPT ratio, and 250Hz CPT ratio were not statistically significant ( $p > 0.05$ ). However, age, 5Hz CPT ratio, and preoperative NRS showed significant differences ( $p < 0.05$ ) between the two groups. Detailed information can be referenced in [Table 1](#). Additionally, there was no significant difference ( $p > 0.05$ ) observed between the test and training groups in terms of gender, age, comorbid hypertension, disease duration, BMI, number of ganglion segments involved, side of the rash, 2000Hz CPT ratio, 250Hz CPT ratio, 5Hz CPT ratio, and preoperative NRS score. Further details are presented in [Table 2](#).

**Table 1** Comparison of General Data of Patients with Different Prognoses of AHN After PRF

Variables	Non-PHN (n = 61)	PHN (n = 45)	Statistic	p
BMI	23.96 ± 2.76	23.49 ± 3.91	t=0.72	0.473
Duration	15.00 (6.00, 30.00)	20.00 (10.00, 30.00)	Z=-1.73	0.084
2000Hz CPT ratio	1.21 (1.04, 1.51)	1.25 (1.12, 1.41)	Z=-1.13	0.259
250Hz CPT ratio	1.22 (1.05, 1.42)	1.35 (1.11, 1.68)	Z=-1.89	0.059
5Hz CPT ratio	1.19 (1.07, 1.38)	1.56 (1.24, 1.89)	Z=-4.64	<0.001
NLGS	3.00 (3.00, 3.00)	3.00 (3.00, 3.00)	Z=-0.21	0.831
NRS			χ <sup>2</sup> =21.70	<0.001
<6	37 (60.66)	7 (15.56)		
≥6	24 (39.34)	38 (84.44)		
Age			χ <sup>2</sup> =5.78	0.016
<65	45 (73.77)	23 (51.11)		
≥65	16 (26.23)	22 (48.89)		
Gender			χ <sup>2</sup> =0.57	0.451
Male	24 (39.34)	21 (46.67)		
Female	37 (60.66)	24 (53.33)		
Hypertension			χ <sup>2</sup> =2.65	0.103
No	42 (68.85)	24 (53.33)		
Yes	19 (31.15)	21 (46.67)		
Side			χ <sup>2</sup> =0.02	0.882
Left	28 (45.90)	20 (44.44)		
Right	33 (54.10)	25 (55.56)		

**Notes:** Results are expressed as mean ± SD, number(percentage), or as median (IQRs).

**Abbreviations:** CPT, current perception threshold; NRS, numeric rating scales; PHN, postherpetic neuralgia; BMI, body mass index, NLGS, number of lesioned ganglion segments.

**Table 2** Comparison of General Information Between Training and Validation Sets

Variable	Train set (n = 74)	Valid set (n = 32)	Statistic	p
2000Hz CPT ratio	1.23 (1.08–1.48)	1.25 (1.10–1.52)	Z=0.585	0.559
250Hz CPT ratio	1.27 (1.07–1.55)	1.24 (1.05–1.61)	Z=0.114	0.910
5Hz CPT ratio	1.25 (1.15–1.66)	1.34 (1.09–1.59)	Z=0.162	0.872
NLGS	3.00 (3.00–3.00)	3.00 (3.00–3.00)	Z=1.731	0.212
BMI	23.54 ± 3.00	24.26 ± 3.88	t=-1.030	0.306
Duration	20.00 (7.00–30.00)	15.00 (7.00–30.00)	Z=0.047	0.964

(Continued)

**Table 2** (Continued).

Variable	Train set (n = 74)	Valid set (n = 32)	Statistic	p
Gender			$\chi^2=1.069$	0.301
Male	29 (39.19)	16 (50.00)		
Female	45 (60.81)	16 (50.00)		
Hypertension			$\chi^2=0.163$	0.687
No	47 (63.51)	19 (59.38)		
Yes	27 (36.49)	13 (40.62)		
Side			$\chi^2=0.401$	0.526
Left	35 (47.30)	13 (40.62)		
Right	39 (52.70)	19 (59.38)		
Age			$\chi^2=0.544$	0.461
<65	45 (60.81)	17 (53.12)		
≥65	29 (39.19)	15 (46.88)		
NRS			$\chi^2=3.382$	0.066
<6	35 (47.30)	9 (28.12)		
≥6	39 (52.70)	23 (71.88)		

**Notes:** Results are expressed as mean ± SD, number(percentage), or as median (IQRs).

**Abbreviations:** CPT, current perception threshold; NRS, numeric rating scales; BMI, body mass index, NLGS, number of lesioned ganglion segments.

## Risk Factors for PRF Prognosis in Patients with AHN

A univariate logistic regression was conducted to determine the correlation between the occurrence of PHN and various independent variables among patients with AHN. The independent variables included age, sex, side of rash, presence of comorbid hypertension, preoperative NRS score, 2000Hz CPT ratio, 250Hz CPT ratio, and 5Hz CPT ratio. The results of the univariate analysis revealed significant associations between age, preoperative NRS score, and 5Hz CPT ratio with the development of PHN after PRF treatment ( $p < 0.05$ ). Conversely, there was no statistically significant correlation found between PHN and gender, side of the rash, presence of hypertension, 2000 hz CPT ratio, and 250 hz CPT ratio ( $p > 0.05$ ). Detailed information can be found in [Table 3](#). Subsequently, a multivariate logistic regression analysis was conducted using stepwise regression with a significance level of  $p < 0.2$  based on the results of the univariate analysis. The study identified the preoperative NRS score (OR = 9.57, 95% CI: 2.68–34.13,  $p < 0.001$ ), age (OR = 3.65, 95% CI: 1.02–13.05,  $p = 0.047$ ), and 5 hz CPT ratio (OR = 8.7, 95% CI: 1.80–42.06,  $p = 0.007$ ) as independent factors influencing the prognosis of PRF treatment in AHN patients. Additional information is provided in [Table 4](#).

## Predictive Value of CPT for PRF Prognosis

The study analyzed the discriminative potential of the 5Hz CPT ratio by plotting the ROC curve, where it served as the independent variable, and the presence or absence of PHN was considered as the dependent variable. The calculated area under the curve (AUC) was 0.764 (95% CI: 0.674–0.855,  $p = 0.003$ ), indicating its predictive accuracy. The best cut-off value was identified as 1.331, highlighting the significance of the 5Hz CPT ratio in distinguishing between patients with varying prognoses. For further information on the results, refer to [Figure 1](#).

**Table 3** The Univariate Logistic Regression Analysis of Prognostic Factors Influencing PRF in Patients with AHN

Variables	Beta	S. E	Z	p	OR (95% CI)
2000Hz CPT ratio	0.78	0.57	1.36	0.173	2.18 (0.71–6.73)
250Hz CPT ratio	0.37	0.55	0.68	0.495	1.45 (0.50–4.27)
5Hz CPT ratio	2.16	0.72	2.98	0.003	8.68 (2.10–35.90)
Gender Female	0.09	0.49	0.18	0.859	1.09 (0.42–2.84)
Hypertension	0.34	0.49	0.70	0.483	1.41 (0.54–3.70)
Side left	0.52	0.48	1.09	0.278	1.68 (0.66–4.32)
Age ≥65	1.08	0.50	2.15	0.031	2.95 (1.10–7.88)
NRS ≥6	2.26	0.58	3.87	<0.001	9.60 (3.05–30.19)

**Abbreviations:** CPT, current perception threshold; NRS, numeric rating scales.

**Table 4** The Multivariate Logistic Regression Analysis of Prognostic Factors Influencing PRF in Patients with AHN

Variables	Beta	S. E	Z	p	OR (95% CI)
2000Hz CPT ratio	0.95	0.75	1.26	0.208	2.58 (0.59–11.27)
5Hz CPT ratio	2.16	0.80	2.69	0.011	8.70 (1.80–42.06)
Age ≥65	1.29	0.65	1.99	0.040	3.65 (1.02–13.05)
NRS ≥6	2.26	0.65	3.48	<0.001	9.57 (2.68–34.13)

**Abbreviations:** CPT, current perception threshold; NRS, numeric rating scales.

## The Nomogram Prediction Model Construction

The nomogram model created using the results of stepwise regression analysis is depicted in [Figure 2](#). This model considers age, preoperative NRS score, and 5-Hz CPT ratio as independent variables to predict the risk of developing PHN after PRF. By summing the scores of each risk factor on the scale provided, the nomogram calculates a total score that reflects the patient's prognosis after PRF. A higher total score on the nomogram signifies an increased probability of a poor postoperative outcome. Thus, the nomogram serves as a tool to predict the likelihood of a poor prognosis following PRF based on specific patient characteristics.

## Evaluation of Nomogram Performance

The prediction accuracy of the nomogram model was evaluated using ROC curves. [Figures 3](#) and [4](#) illustrate that the AUC of the ROC curve was 0.863 (95% CI, 0.776–0.950) for the training group and 0.859 (95% CI, 0.721–0.998) for the validation group. These results confirm the model's good discriminative ability in both the training and validation sets. In the training set, the calibration curves demonstrate a close alignment between the predicted and measured values. The Hosmer-Lemeshow goodness-of-fit test yielded a non-significant result ( $p > 0.05$ ), indicating a strong fit of the model to the observed data, as shown in [Figure 5](#). Similarly, the validation dataset produced consistent findings, with the predicted values closely matching the measured values. The non-significant Hosmer-Lemeshow goodness-of-fit test ( $p > 0.05$ ) in this dataset further affirms the model's adequacy in fitting the observed data, as depicted in [Figure 6](#). DCA analysis was then conducted on the selected predictor variables for poor postoperative prognosis using the nomogram prediction model. The results, presented in [Figure 7](#), revealed that the nomogram was particularly advantageous in predicting the risk of poor postoperative prognosis following PRF in AHN patients when the threshold probability ranged from 0 to 0.820. This broader range of selectable threshold probabilities underscores the model's robust assessment capabilities.

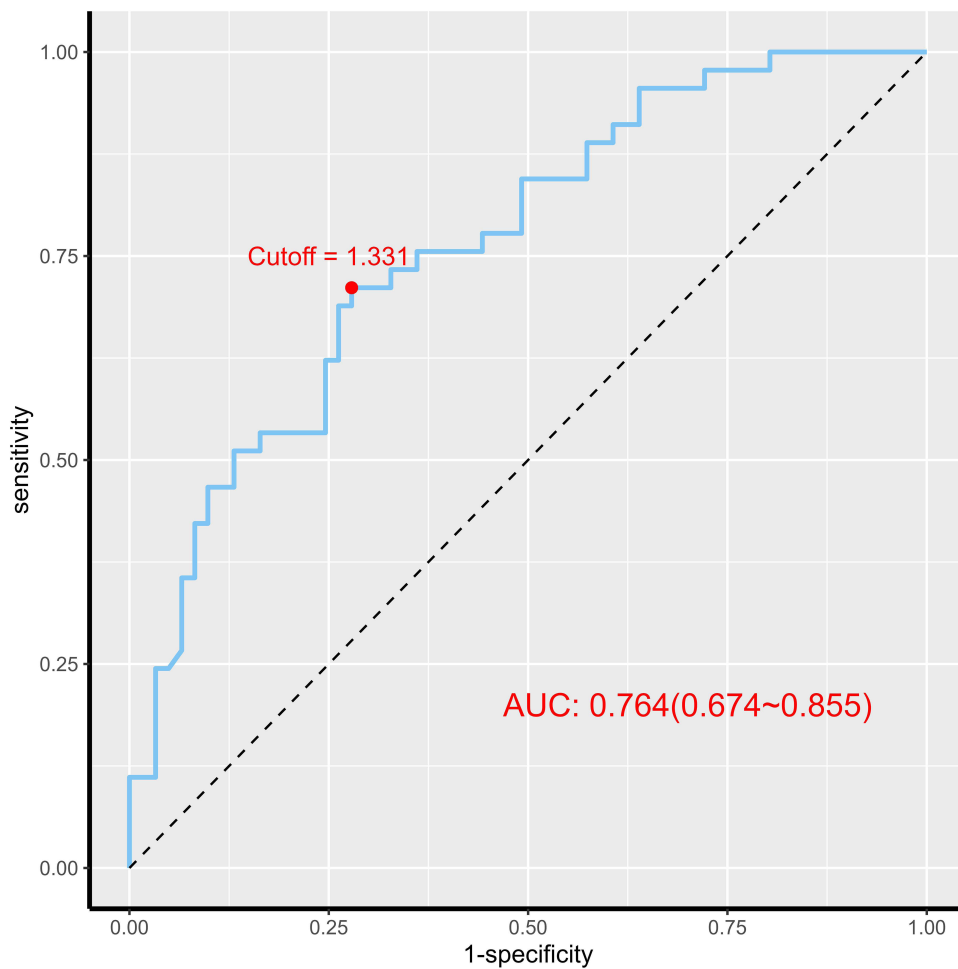


**Figure 1** The receiver operating characteristic (ROC) curve of 5Hz CPT ratio to predict the prognosis of AHN after PRF.

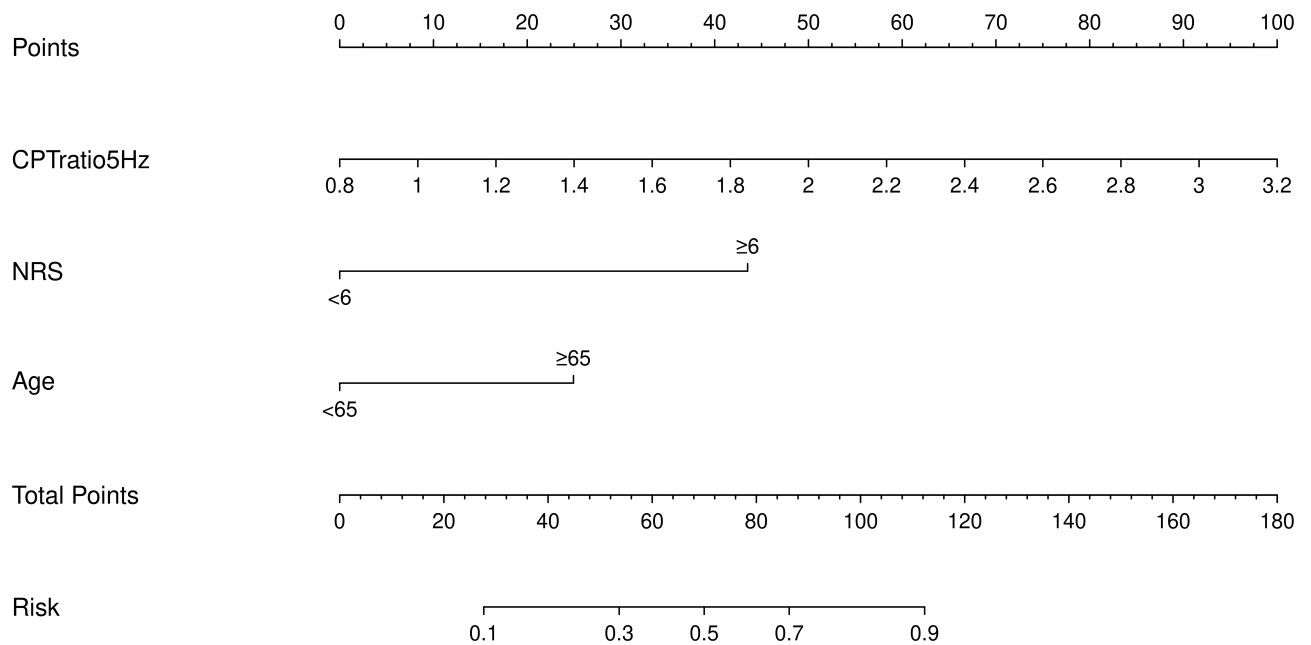


**Figure 2** The nomogram to predict the prognosis of PRF in patients with AHN.

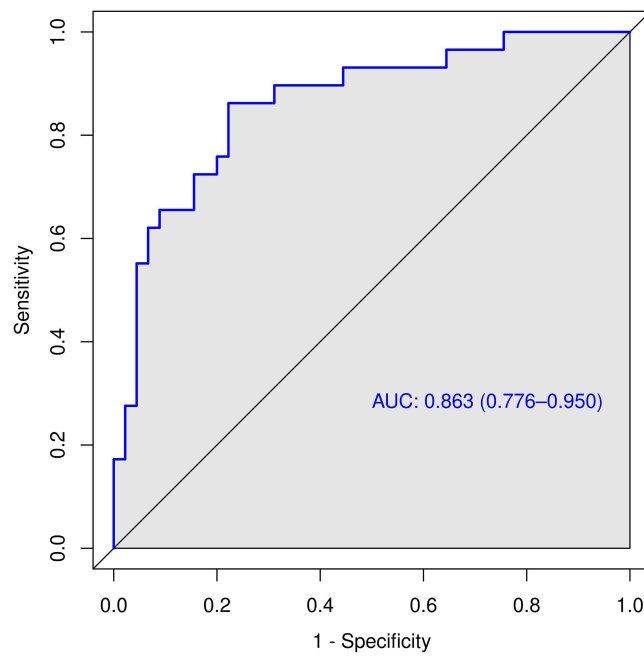


**Figure 3** ROC curve of the nomogram for predicting the prognosis of PRF in patients with AHN in the train set.

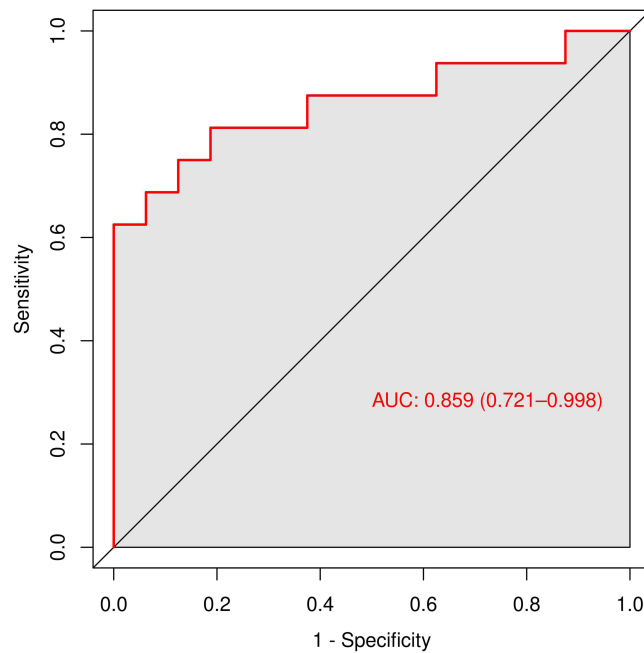


**Figure 4** ROC curve of the nomogram for predicting the prognosis of PRF in patients with AHN in the valid set.

## Discussion

The study results reveal that the 5Hz CPT index can effectively predict the prognosis of PRF in individuals with AHN. Independent risk factors associated with poor prognosis of PRF in patients with HZ on the thoracic back during the acute phase include age, preoperative NRS score, and preoperative 5Hz CPT ratio. Specifically, patients aged 65 years or older, presenting with a preoperative NRS score of 6 or higher, and exhibiting a higher 5Hz CPT ratio were found to have a more unfavorable prognosis for pulsed radiofrequency treatment. Notably, no significant associations were observed between prognosis and the 2000Hz CPT ratio or the 250Hz CPT ratio, as well as the patient’s sex, side of the rash, or



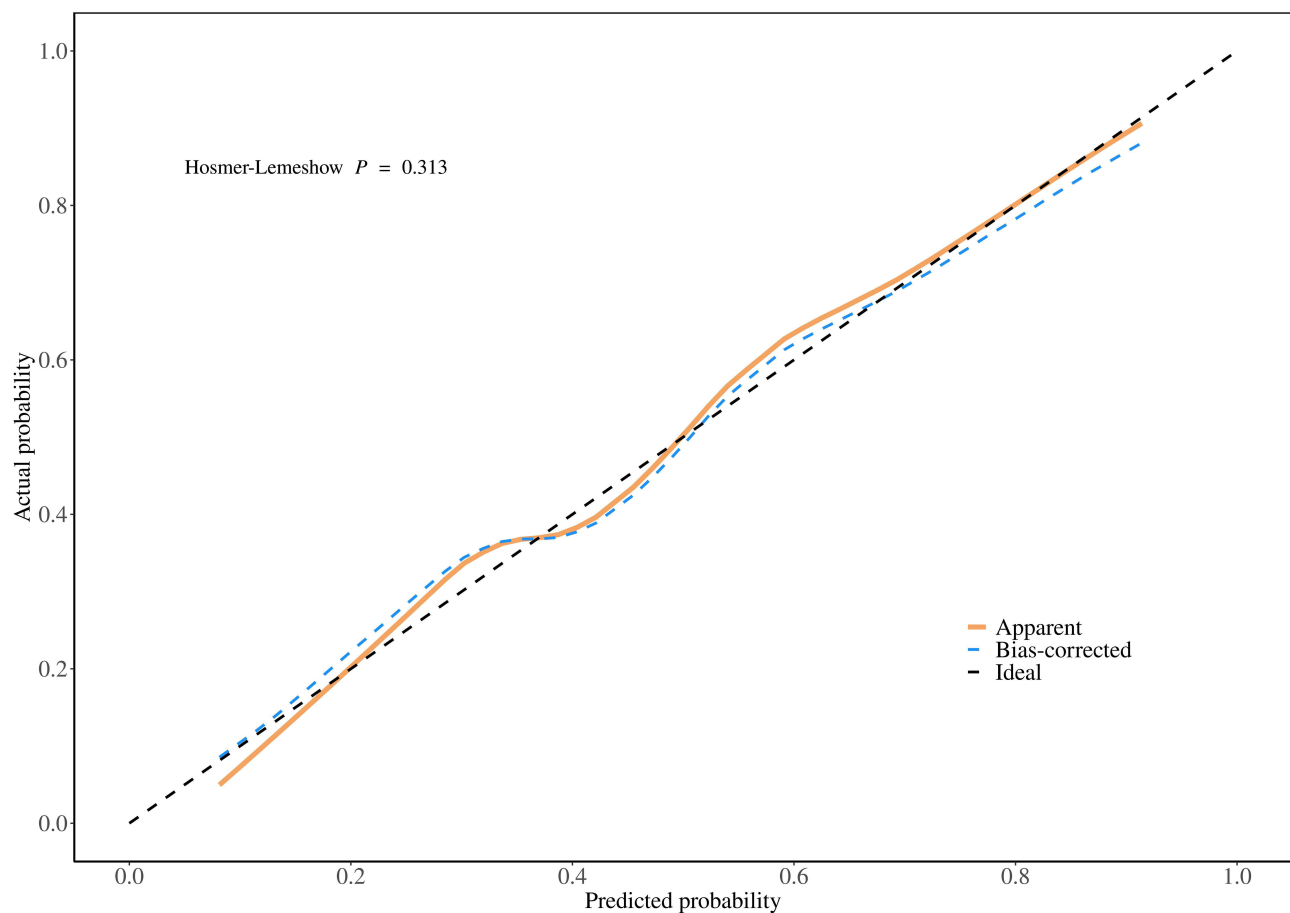


**Figure 5** The calibration curve of nomogram model in the train set.

presence of hypertension. These results emphasize the importance of early screening of patients with potential poor PRF treatment prognosis to enable adjustments in the treatment strategy or incorporation of interventions aimed at achieving improved clinical outcomes.

PRF is a neuromodulation technique known for its advantages, such as no nerve damage, high safety factor, and minimal complications. The specific analgesic mechanism of PRF remains incompletely understood. In a study conducted by Protasoni, the rat dorsal root ganglion (DRG) underwent a 30-second PRF treatment, and immediate changes in DRG tissue structure were examined through light and electron microscopy after just one hour.<sup>19</sup> The study revealed that myelinated axons exhibited pathological alterations, whereas unmyelinated axons maintained their normal morphology and size. This observation suggested that PRF induced structural modifications in myelinated nerve fibers within the DRG, potentially contributing to its analgesic effects. Additionally, an animal experiment demonstrated that PRF could alleviate neuropathic pain by suppressing substance P expression in the spinal cord.<sup>20</sup> Furthermore, Li discovered that pulsed radiofrequency elevated plasma  $\beta$ -endorphin levels, which might be associated with the analgesic actions of PRF.<sup>21</sup> Another animal study found that PRF had the potential to reverse nerve demyelination and support nerve regeneration.<sup>22</sup> Nonetheless, the complete extent of its capability to reverse nerve damage remains unclear. Consequently, it is plausible that the severity of sensory nerve damage could serve as a predictor for the prognosis of PRF therapy. Our research approach involved utilizing the CPT ratio of the unaffected side to objectively evaluate nerve injury on the affected side. The findings indicated that the 5-Hz CPT ratio exhibited a degree of predictive utility for the prognosis of PRF (AUC=0.764, 95% CI: 0.674–0.855).

Elderly patients with AHN, aged 65 years or older, and presenting with a preoperative NRS score of 6 or higher are at an increased risk of poor prognosis, corroborating previous studies on herpes zoster.<sup>23,24</sup> The probability of viruses latent

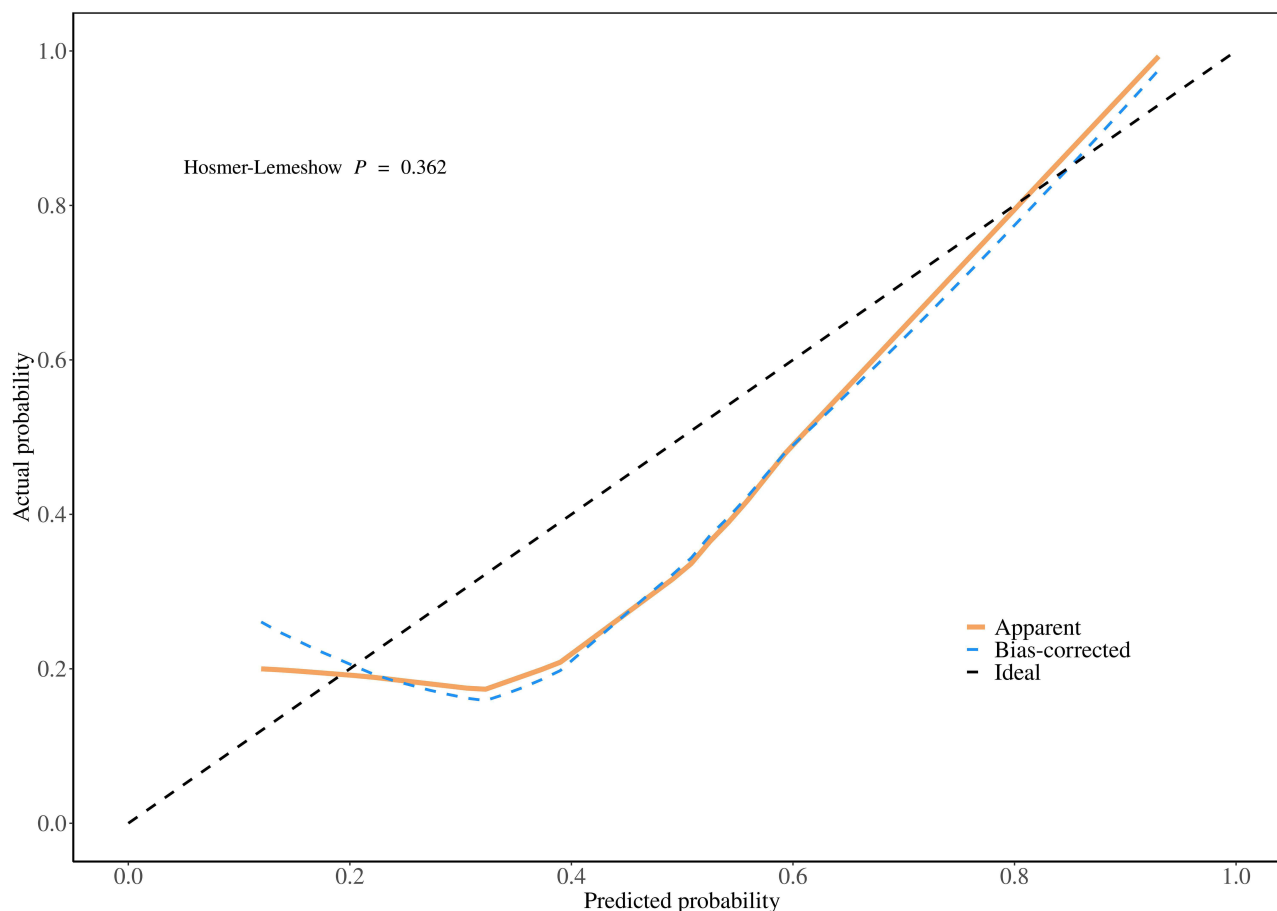


**Figure 6** The calibration curve of nomogram model in the valid set.

in the nerves reactivating during early life is commonly linked to diminished immune function, thereby heightening the probability of developing PHN. Notably, advancing age frequently results in varying degrees of immune function decline within the body.<sup>25</sup> Furthermore, the elderly population is more vulnerable to viral infections and may exhibit accelerated neurological deterioration, consequently escalating the likelihood of an unfavorable prognosis in PRF.

Preoperative NRS score is another risk factor that affects the prognosis of PRF. Severe and persistent pain can have many psychological effects, such as insomnia, anorexia, and irritability. As some patients may not experience complete pain resolution after surgery, psychological factors may negatively impact their prognosis. Additionally, severe pain may indicate a high degree of nerve damage. Acute phase pain is caused by the activation of latent VZV, which replicates in large numbers and proliferates rapidly, leading to necrosis of nerve fibers as a neuroimmune response.<sup>26</sup> Stein investigated the process of VZV activation in human ganglia. They found evidence of an immune response to ganglion and nerve fiber involvement, with ganglia showing necrosis and hemorrhage, and heavy infiltration of CD4+ and CD8+ T cells in both ganglia and nerve fibres.<sup>27</sup> Additionally, they observed upregulation of the expression of major histocompatibility complex (MHC-I and MHC-II) molecules on glial cells. The severity of the inflammatory response, nerve fiber damage, and destruction, as well as the signs and symptoms of neuralgia, are directly proportional to the intensity of pain experienced during the acute phase. Higher pain scores indicate a more severe condition, and these patients require urgent surgery and tend to have higher expectations of outcomes.<sup>28</sup> Therefore, the use of pulsed radiofrequency alone may not be sufficient to restore neurological function and may increase the risk of poor prognosis.

The Neurometer<sup>®</sup> CPT/C Sensory Nerve Quantification Tester is employed in conducting the CPT assay, which is designed to identify sensory nerve functionality at distinct skin locations. This tester operates at three different frequencies: 2000 hz, 250 hz, and 5 hz, transmitting electrical stimuli to assess the functional status of A $\beta$ , A $\delta$ , and

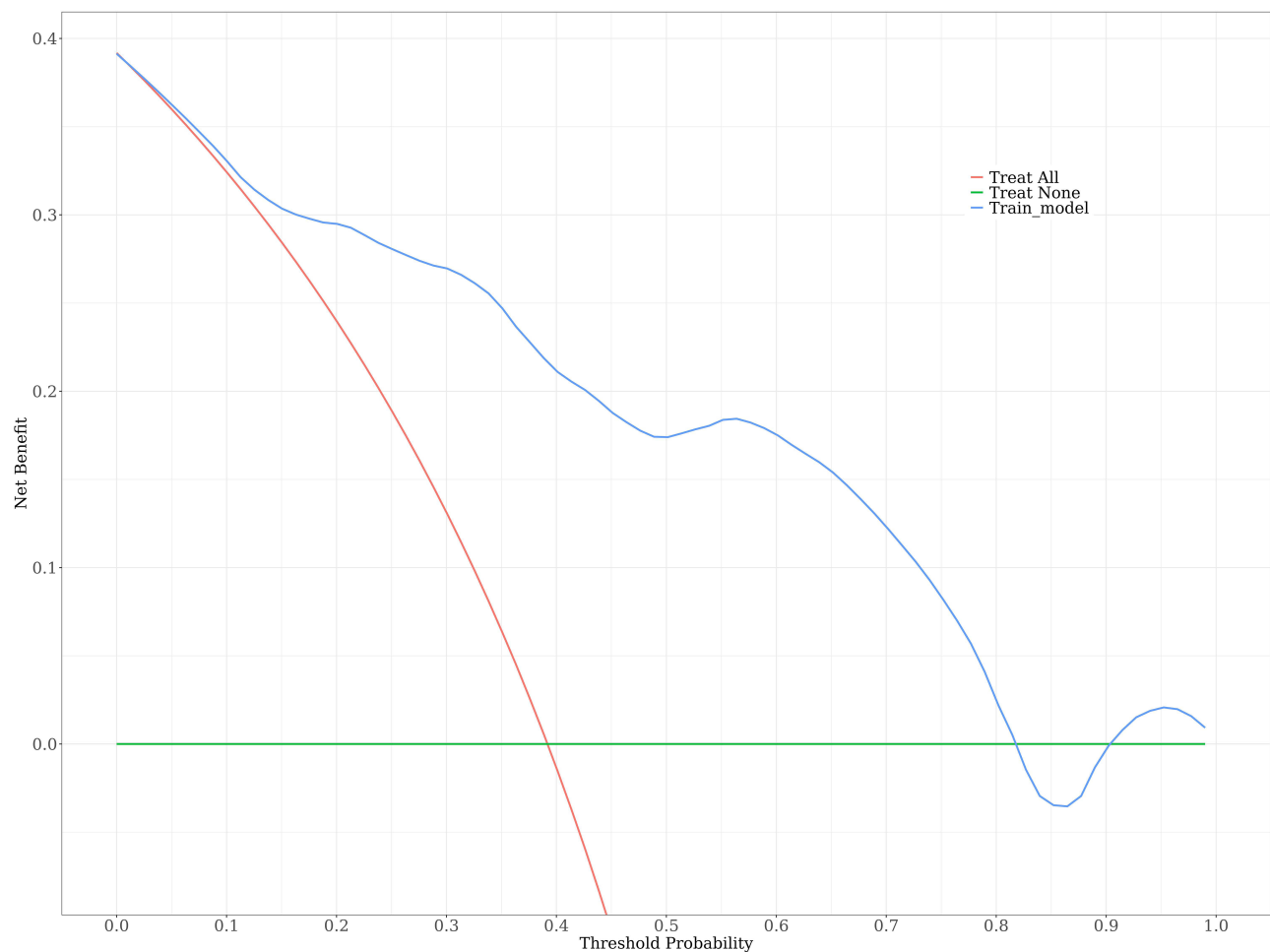


**Figure 7** The decision curve analysis (DCA) of the nomogram for predicting prognosis in PRF.

C nerve fibers.<sup>29</sup> Through the data report generated by the device, the operator can quantitatively evaluate the extent of nerve impairment on the impacted side. Elevated CPT values typically indicate a positive correlation with the severity of nerve damage. In 1995, Watkins discovered demyelinating damage to the affected brachial plexus nerves in patients with HZ.<sup>30</sup> In 2010, Gowrishankar observed persistent neuronal antibodies to VZV in sensory ganglia of deceased patients with HZ.<sup>31</sup> It has been suggested that hypoesthesia is associated with an increased risk of PHN.<sup>32</sup> Additionally, the results indicate that a high 5 hz CPT ratio is a risk factor for the prognosis of PRF treatment, which is consistent with previous research. The reason for the lack of significant correlation between the 2000 hz ratio or 250 hz ratio and PRF prognosis could be attributed to the virus selectively invading C unmyelinated fibers, which represent the majority of nerve fibers at 80–90%, while A $\beta$  and A $\delta$  myelinated nerve fibers only account for 10%. This discrepancy underscores the importance of the 5 hz CPT ratio, as a larger difference between the affected and healthy sides indicates a more pronounced nerve damage, potentially leading to reduced effectiveness of pulsed radiofrequency neuromodulation and an elevated risk of developing PHN.

The study employed univariate and multivariate logistic regression analyses to identify clinically significant variables, thus constructing a formal nomogram for personalized predictive analysis of clinical events. It aimed to create a more accurate risk assessment model compared to traditional statistical methods.<sup>33</sup> To assess the model's performance, we randomly assigned eligible patients into a training group (n=74) and a validation group (n=32). The training group exhibited high performance, achieving an AUC of 0.861 in predicting the ROC curve represented by the model. Subsequently, the validation phase confirmed the reliability of the predictive model by showcasing good performance

across high sensitivity, calibration, and clinical utility. Overall, these results demonstrate the nomogram's effectiveness in accurately predicting clinical outcomes.

Among the 45 patients who developed a poor prognosis, 27 patients underwent repetitive high-voltage long-duration pulsed radiofrequency, 10 received radiofrequency thermocoagulation, 3 underwent spinal cord stimulation, and 5 declined further treatment. All patients who received follow-up treatment demonstrated significant pain relief.

## Limitations

This study has some limitations that need to be addressed. Firstly, due to the retrospective nature of the study, there is a lack of continuous and dynamic CPT data, making it unclear whether CPT indexes change with the condition of treated AHN patients. Secondly, the small sample size may have limited the ability of the univariate and multivariate regression analyses to account for other potential risk factors that could influence the prognosis of PRF treatment and may result in potential bias. Thirdly, the relatively small sample size may limit the generalizability of the findings to non-Asian populations. Consequently, further validation in non-Asian populations is required. Finally, the constructed model lacks external validation, highlighting the necessity for further prospective multicenter large-sample studies to validate the model.

## Conclusions

The present investigation revealed that the 5Hz CPT ratio is a significant predictor of treatment outcomes after PRF therapy in individuals suffering from AHN. Notably, an elevated 5Hz CPT ratio is associated with an increased likelihood of PHN occurrence. In addition, the study successfully formulated and validated an accurate prognostic nomogram model. Consequently, this model offers a valuable tool for early detection and screening of unfavorable prognostic outcomes post-radiofrequency treatment in patients with AHN.

## Acknowledgments

Each author has contributed significantly to the work presented in this manuscript, whether through the initial concept and design, the execution and management of the study, the analysis and interpretation of the data, or across all these dimensions. They have been involved in the drafting, revision, or provided critical feedback on the article; have given their final approval for the version to be published; have concurred on the choice of journal for submission; and have acknowledged their responsibility for every facet of the work.

## Disclosure

The authors report no conflicts of interest in this work.

## References

1. Van Oorschot D, Vroiling H, Bunge E, Diaz-Decaro J, Curran D, Yawn B. A systematic literature review of herpes zoster incidence worldwide. *Hum Vaccines Immunother.* 2021;17(6):1714–1732. doi:10.1080/21645515.2020.1847582
2. Opstelten W, McElhaney J, Weinberger B, Oaklander AL, Johnson RW. The impact of varicella zoster virus: chronic pain. *J Clin Virol.* 2010;48 Suppl 1:S8–13. doi:10.1016/S1386-6532(10)70003-2
3. Gross GE, Eisert L, Doerr HW, et al. S2k guidelines for the diagnosis and treatment of herpes zoster and postherpetic neuralgia. *J der Deutschen Dermatologischen Gesellschaft.* 2020;18(1):55–78 doi:10.1111/ddg.14013.
4. Johnson RW. Consequences and management of pain in herpes zoster. *J Infect Dis.* 2002;186 Suppl 1:S83–90. doi:10.1086/342970
5. Chen LK, Arai H, Chen LY, et al. Looking back to move forward: a twenty-year audit of herpes zoster in Asia-Pacific. *BMC Infect Dis.* 2017;17(1):213 doi:10.1186/s12879-017-2198-y.
6. Klompas M, Kulldorff M, Vilk Y, Bialek SR, Harpaz R. Herpes zoster and postherpetic neuralgia surveillance using structured electronic data. *Mayo Clin Proc.* 2011;86(12):1146–1153. doi:10.4065/mcp.2011.0305
7. Díez-Domingo J, Curran D, Cambronero MDR, Garcia-Martinez JA, Matthews S. Economic burden and impact on quality of life of Herpes Zoster in Spanish adults aged 50 years or older: a prospective cohort study. *Adv ther.* 2021;38(6):3325–3341. doi:10.1007/s12325-021-01717-7
8. Hunter P. Getting tough on pain. The potential of painkillers that take aim at chronic pain in smart new ways. *EMBO Rep.* 2013; 14(3):236–238. doi:10.1038/embo.2013.12
9. Flor, H. Painful memories. Can we train chronic pain patients to 'forget' their pain? *EMBO Rep.* 2002 ;3(4):288–291 doi:10.1093/embo-reports/kvf080

10. Finnerup NB, Kuner R, Jensen TS. Neuropathic pain: from mechanisms to treatment. *Physiol Rev.* 2021;101(1):259–301. doi:10.1152/physrev.00045.2019
11. Binder A, Baron R. The pharmacological therapy of chronic neuropathic pain. *Deutsches Arzteblatt International.* 2016;113(37):616–625. doi:10.3238/arztebl.2016.0616
12. Huang X, Ma Y, Wang W, Guo Y, Xu B, Ma K. Efficacy and safety of pulsed radiofrequency modulation of thoracic dorsal root ganglion or intercostal nerve on postherpetic neuralgia in aged patients: a retrospective study. *BMC Neurol.* 2021;21(1):233. doi:10.1186/s12883-021-02286-6
13. Moussa WM, Khedr W, Elsayy M. Percutaneous pulsed radiofrequency treatment of dorsal root ganglion for treatment of lumbar facet syndrome. *Clin Neurol Neurosurg.* 2020;199:106253. doi:10.1016/j.clineuro.2020.106253
14. Li HQ, Xia LJ, Jiang YH, et al. Efficacy and safety of pulsed radiofrequency combined with gabapentin in the treatment of acute herpetic neuralgia. *Zhonghua Yi Xue Za Zhi.* 2023;103(48):3954–3958. doi:10.3760/cma.j.cn112137-20230921-00517
15. Kurihara K, Fujioka S, Mishima T, Tsuboi Y. Evaluation of perception threshold and pain in patients with Parkinson's disease using PainVision<sup>®</sup>. *Front Neurol.* 2023;14:1130986. doi:10.3389/fneur.2023.1130986
16. Tordai DZ, Hajdú N, Rácz R, et al. Genetic factors associated with the development of neuropathy in type 2 diabetes. *Int J Mol Sci.* 2024;25(3):1815. doi:10.3390/ijms25031815
17. Uddin Z, MacDermid JC, Galea V, Gross AR, Pierrynowski MR. The current perception threshold test differentiates categories of mechanical neck disorder. *The J Ortho Sports Phys Ther.* 2014;44(7):532–540. doi:10.2519/jospt.2014.4691
18. Seok HY, Cho YW. Long-term dopamine agonist treatment fails to restore altered central sensory processing in restless legs syndrome: evidence from current perception threshold measurements. *Sleep Med.* 2024;113:1–5. doi:10.1016/j.sleep.2023.11.010
19. Protasoni M, Reguzzoni M, Sangiorgi S, et al. Pulsed radiofrequency effects on the lumbar ganglion of the rat dorsal root: a morphological light and transmission electron microscopy study at acute stage. *Eur Spine J.* 2009;18(4):473–478. doi:10.1007/s00586-008-0870-z
20. Wang JA, Niu SN, Luo F. Pulsed radiofrequency alleviated neuropathic pain by downregulating the expression of substance P in chronic constriction injury rat model. *Chinese Med J.* 2020;133(2):190–197. doi:10.1097/CM9.0000000000000619
21. Li D, Sun G, Sun H, Wang Y, Wang Z, Yang J. Combined therapy of pulsed radiofrequency and nerve block in postherpetic neuralgia patients: a randomized clinical trial. *PeerJ.* 2018;6:e4852. doi:10.7717/peerj.4852
22. Li DY, Meng L, Ji N, Luo F. Effect of pulsed radiofrequency on rat sciatic nerve chronic constriction injury: a preliminary study. *Chinese Med J.* 2015;128(4):540–544. doi:10.4103/0366-6999.151113
23. Hu J, Zhong LZ, Li TT, Jia QY, Li HM. Study of risk factors of postherpetic neuralgia. *Zhonghua Yi Xue Za Zhi.* 2022;102(40):3181–3185. doi:10.3760/cma.j.cn112137-20220601-01213
24. Peng Z, Guo J, Zhang Y, et al. Development of a model for predicting the effectiveness of pulsed radiofrequency on zoster-associated pain. *Pain Ther.* 2022;11(1):253–267. doi:10.1007/s40122-022-00355-3
25. Petersen KL, Rice FL, Farhadi M, Reda H, Rowbotham MC. Natural history of cutaneous innervation following herpes zoster. *Pain.* 2010;150(1):75–82. doi:10.1016/j.pain.2010.04.002
26. Saguil A, Kane S, Mercado M, Lauters R. Herpes zoster and postherpetic neuralgia: prevention and management. *Am Family Phys.* 2017;96(10):656–663 PMID: 29431387.
27. Steain M, Sutherland JP, Rodriguez M, Cunningham AL, Slobedman B, Abendroth A. Analysis of T cell responses during active varicella-zoster virus reactivation in human ganglia. *J Virol.* 2014;88(5):2704–2716. doi:10.1128/JVI.03445-13
28. Ito S, Yasuda M, Kondo H, et al. Clinical courses of herpes simplex virus-induced urethritis in men. *J Infect Chemother.* 2017;23(10):717–719. doi:10.1016/j.jiac.2017.03.017
29. Ghazi AA, Abuzgaya M, Banakhar M, Hassouna M. The role of the neurometer CPT/C in sacral neuromodulation. *Turkish j Urol.* 2018;44(1):70–74. doi:10.5152/tud.2017.81592
30. Watkins LR, Maier SF, Goehler LE. Immune activation: the role of pro-inflammatory cytokines in inflammation, illness responses and pathological pain states. *Pain.* 1995;63(3):289–302. doi:10.1016/0304-3959(95)00186-7
31. Gowrishankar K, Steain M, Cunningham AL, et al. Characterization of the host immune response in human Ganglia after herpes zoster. *J Virol.* 2010;84(17):8861–8870. doi:10.1128/JVI.01020-10
32. Kramer S, Baeumler P, Geber C, et al. Somatosensory profiles in acute herpes zoster and predictors of postherpetic neuralgia. *Pain.* 2019;160(4):882–894. doi:10.1097/j.pain.0000000000001467
33. Juan X, Jiali H, Ziqi L, Liqing Z, Han Z. Development and validation of nomogram models for predicting postoperative prognosis of early-stage laryngeal squamous cell carcinoma. *Current Prob Cancer.* 2024;49:101079. doi:10.1016/j.currprobcancer.2024.101079